LANGMUIR

Article

pubs.acs.org/Langmuir

Stimuli-Responsive Polyoxometalate/Ionic Liquid Supramolecular Spheres: Fabrication, Characterization, and Biological Applications

Yanjun Gong,[†] Qiongzheng Hu,[‡] Chen Wang,[§] Ling Zang,[§] and Li Yu*[,†]

[†]Key Laboratory of Colloid and Interface Chemistry, Ministry of Education, Shandong University, Jinan 250100, P. R. China

[‡]Department of Chemistry, University of Houston, Houston, Texas 77204, United States

[§]Nano Institute of Utah and Department of Materials Science and Engineering, University of Utah, Salt Lake City, Utah 84112, United States

Supporting Information

ABSTRACT: We report fabrication, characterization, and potential applications of polyoxometalate (POM)/ionic liquid (IL) supramolecular spheres in water for the first time. These supramolecular spheres have highly ordered structures and show excellent reversible self-assembly and tunable photoluminescence properties, which can be manipulated by adjusting pH of the aqueous solution. Specifically, the formation of POM/IL supramolecular spheres results in quenching of fluorescence emitted by Eu-POM because hopping of the d_1 electron in the POM molecule is blocked by hydrogen bond existing between the oxygen atom of POM and the carboxylic acid group of IL. However, the fluorescence can be completely recovered by gradually increasing pH of the aqueous solution due to the pH-induced deprotonation of the carboxylic acid group of IL, which results in disassembly of the fabricated supramolecular spheres. Applications of these stimuli-responsive photoluminescent POM-based supramolecular materials are demonstrated in biological media. Dual signaling responses of turbidity and fluorescence are observed simultaneously in the detection of urease and heavy metals based on pH-induced disassembly of the supramolecular spheres during the biochemical events in aqueous solution. In addition, guest molecules are encapsulated into the supramolecular spheres, and controlled release of these entrapped molecules is demonstrated in the presence of external stimuli. This study shows potential of stimuli-responsive POM/IL supramolecular materials in biological applications.

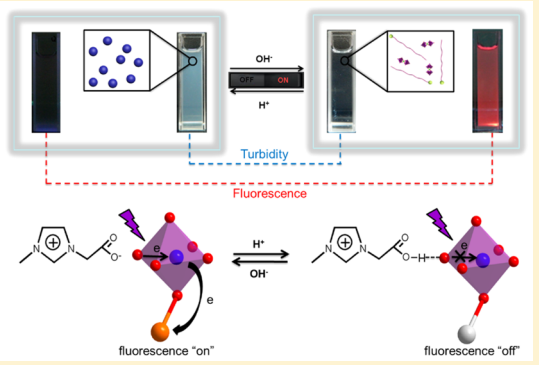

1. INTRODUCTION

Supramolecular self-assembly is widely applied in rationally designing varieties of multifunctional materials.[1−5] Among them, stimuli-responsive self-assemblies have drawn particular attention due to feasibility of modulating structures, morphologies, and functions of these materials in the presence of external stimuli.[6−9] Polyoxomylatates (POMs) are typical clusters of nanometer-sized transition metal oxide that are emerging as useful materials for potential applications in diverse fields such as catalysis, material science, and sensing, etc.[10−14] They are always applied as anionic nanoscale building blocks for construction of self-assembled nanostructured composites or hybrid inorganic−organic materials.[15−19] For example, Li et al. demonstrated the fabrication of onion-like hybrid assemblies based on surfactant-encapsulated clusters (SECs) of POMs in organic solvents.[20] Rickert et al. reported synthesis of the POM-based ionic liquids (ILs) by partial replacement of protons of POMs with cations of ILs.[21]

Although self-assembling of supramolecular materials with different structures has been extensively investigated for multifunctional applications,[22−25] it is still quite attractive to construct stimuli-responsive POM-based supramolecular materials with multiple functions such as reversible self-assembly and well-controlled photoluminescence in aqueous solution, which may expand the potential applications of these materials. In particular, despite various studies involving POMs containing lanthanides such as europium in the solid state or organic media, practical applications of these materials remain limited in biological media.[26−28] Therefore, development of stimuli-responsive POM-based supramolecular materials with enhanced photoluminescence in aqueous solution is highly desirable for a wide range of biological applications such as sensing and controlled drug release. Besides, POM clusters are mainly employed as molecular catalysts or labels in sensing applications.[29−32] However, only a quite limited number of analytes can be detected using these methods. Because of diversity, rich structural variety, and unique properties, POM-based supramolecular materials with stimuli-induced responses may be a potent candidate for the sensing applications. Very recently, Wei et al. demonstrated fabrication of specially designed supramolecular chemosensors by using stimuli-responsive POM-based supramolecular materials, which

Received: October 20, 2015
Revised: December 18, 2015
Published: December 24, 2015

DOI: 10.1021/acs.langmuir.5b03883
Langmuir 2016, 32, 421−427

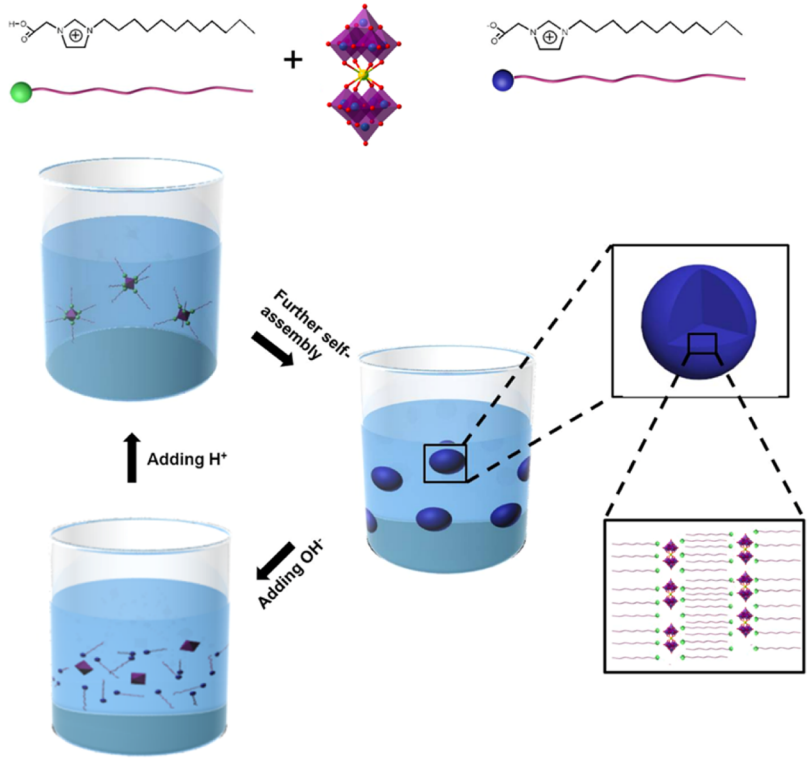

Figure 1. Schematic principle of the pH-reversible self-assembly of Eu-POM/IL supramolecular spheres.

shows promise of these materials.[33] But there is still a lack of studies on the biochemical detection using stimuli-responsive POM-based supramolecular materials.

Herein, we report fabrication and characterization of POM/IL supramolecular spheres with highly ordered structures in water directly with pH-reversible self-assembly behavior and well-controlled photoluminescence responses and demonstrate applications of these stimuli-responsive supramolecular materials in biological environment. Noteworthy is that turbidity- and fluorescence-based assays are applied simultaneously in the study of biochemical interactions, which is attributed to pH-induced disassembly of the supramolecular hybrids. In addition, encapsulation and controlled release of guest molecules can be fulfilled based on responses of the supramolecular spheres to environmental changes. Our study provides a perspective for designing and applying stimuli-responsive POM/IL supramolecular materials in biological applications.

2. EXPERIMENTAL SECTION

2.1. Materials. Europoum nitrate hexanydrate (99%), sodium tungstate dehydrate (99%), and urea (99%) were all purchased from J&K Chemical Technology, China. Urease (100 KU) was bought from Shanghai ZZBio CO., Ltd., of China. 1-Bromododecane (98%), 1-methylimidazole (99%), 1-dodecylimidazole (99%), and bromoacetic acid (99%) were purchased from Aladdin Chemistry Co., Ltd., of China. Methyl orange (99%) and rhodamine 6G (99%) were purchased from J&K Chemical Technology, China. The triply distilled water was prepared by a SZ-97 automatic triple water distiller (Shanghai YR BioChem CO., Ltd., China). All above reagents were used without further purification.

2.2. Synthesis of [N-C_{12}, N′-Im]Br. 1-Methylimidazole (0.1 mol) and 1-bromododecane (0.12 mol) were dissolved in acetonitrile (50 mL), and the mixture was stirred at 75−80 °C under a nitrogen atmosphere for 48 h. The solvent was removed by evaporation under reduced pressure. The product (26 g, yield 78%) was purified by recrystallization from ethyl acetate at least four times and then dried *in vacuo* for 48 h. ^{1}H NMR ($CDCl_3$, δ/ppm): 0.75 (t, 3H, $-CH_3$), 1.18−1.29 (d, 18H, $-(CH_2)_9CH_3$), 1.84 (t, 2H, $-CH_2(CH_2)_9CH_3$), 3.91 (s, 3H, $-NCH_3$), 4.24 (t, 2H, $-CH_2(CH_2)_{10}CH_3$), 7.52 (m, 2H, −NCHCHN−), 9.05 (s, 1H, −NCHN−).

2.3. Synthesis of [N-C_{12}, N′-COOH-Im]Br. [N-C_{12}, N′-COOH-Im]Br was prepared according to previous literature.[34] Briefly, bromoacetic acid (86 mmol) was added to 50 mL of methanol solution of 1-dodecylimidazole (95 mmol) under continuous stirring. The mixture was refluxed at 70 °C for 6 h under the protection of nitrogen. After removing excess methanol, the residue was recrystallized five times by using the methanol/ether mixture to obtain [N-C_{12}, N′-COOH-Im] Br (20 g, yield 63%). ^{1}H NMR (D_2O, δ/ppm): δ = 8.80 (s, 1 H, CH), 7.46 (d, 1 H, CH), 7.46 (d, 1 H, CH), 4.88 (s, 2 H, CH_2), 4.18 (t, 2 H, CH_2), 1.83 (m, 2 H, CH_2), 1.27 (m, 18 H, CH_2), 0.80 (t, 3 H, CH_3). Calcd for [N-C_{12}, N′-COOH-Im]Br: C, 69.40; H, 10.20; O, 10.88; N, 9.52. Found: C, 69.25; H, 10.78; O, 10.72; N, 9.25.

2.4. Preparation of Eu-POM/IL Supramolecular Spheres. $Na_9EuW_{10}O_{36}{\cdot}32H_2O$ was prepared as described by Sugesta and Yamase.[35] Aqueous solutions of Eu-POM (5 mL, 0.5 mM) were injected into [N-C_{12}, N′-COOH-Im]Br (45 mL, 0.5 mM) under ultrasonic state (40 kHz, 100 W) at room temperature. After 30 min, the stable colloidal solutions were formed. Then, the products were collected by a centrifuge and washed three times with water to remove salts and possible precursors. The final products were dried under vacuum at 55 °C for 24 h.

For supramolecular spheres encapsulated with methyl orange (MO) molecules, the MO solution (2.5 mL, 10 M) was added to an aqueous solution of Eu-POM (2.5 mL, 1 mM), and then the mixed solution was injected to the [N-C_{12}, N′-COOH-Im]Br solution (45 mL, 0.5 mM) to form the hybrid colloidal spheres.

For supramolecular spheres encapsulated with rhodamine 6G (R6G) molecules, the R6G solution (2.5 mL, 5 M) was added to an aqueous solution of [N-C_{12}, N′-COOH-Im]Br (45 mL, 0.5 mM). Subsequently, Eu-POM solution (2.5 mL, 1 mM) was injected to the [N-C_{12}, N′-COOH-Im]Br/R6G solution to form the hybrid colloidal spheres.

2.5. Characterization of the Synthesized Supramolecular Spheres. The ^{1}H NMR spectra were recorded using a Bruker AV-300

DOI: 10.1021/acs.langmuir.5b03883
Langmuir 2016, 32, 421−427

NMR spectrometer with a pulse field gradient module (*Z*-axis) and a 5 mm sample tube. The instrument was operated at a frequency of 300.13 MHz at 25 °C with tetramethylsilane as an internal reference. Deuterated dimethyl sulfoxide (DMSO) was selected as the solvent. The elemental analysis measurements were performed on a Vario EL III elementar analyzer (Elementar). The mass analysis data were performed on Agilent 6510Q-TOF. The nanostructures were characterized by transmission electron microscopy (TEM) (JEM-100CX II (JEOL)). Luminescent measurements were performed on a Hitachi F-4500 fluorescence spectrophotometer. 10 μL of the colloidal solution was applied to a carbon-coated copper grid for 3 min after removal of excess solution with filter paper. UV/vis spectra were measured in a quartz cell (light path of 1 cm) by using a HP 8453E instrument. Fourier transform IR (FTIR) spectra were recorded between 4000 and 400 cm^{-1} by using a VERTEX-70/70v FTIR spectrometer (Bruker Optics, Germany) on pressed thin KBr sample disks. Small-angle X-ray scattering (SAXS) measurements were performed using an Anton-paar SAX Sess mc^2 system with a Ni-filtered Cu Kα radiation (1.5406 Å) operated at 50 kV and 40 mA.

3. RESULTS AND DISCUSSION

3.1. Synthesis and Characterization of the Eu-POM/IL Supramolecular Spheres. The Eu-POM/IL supramolecular spheres were prepared by incubating an Eu-containing polyoxomylatate, $Na_9EuW_{10}O_{36}\cdot 32H_2O$, with a COOH-functionalized imidazolium-based IL, *N*-dodecyl-*N*′-carboxymethylimidazolium bromide ([N-C_{12}, N′-COOH-Im]Br) in water. Figure 1 shows a schematic principle of the method. Eu-POM and [N-C_{12}, N′-COOH-Im]Br initially form IL-encapsulated Eu-POM supramolecular complexes through electrostatic interactions and H-bond in water. Subsequently, these supramolecular complexes self-assemble into hybrid spheres due to hydrophobic interactions between long hydrocarbon chains of ILs decorated on the Eu-POM clusters. For the COOH-functionalized IL, the carboxylic acid group deprotonates into the carboxylate anion in the aqueous alkaline solution, inducing disassembly of the supramolecular spheres due to electrostatic repulsions between Eu-POM and the deprotonated IL. Therefore, reversible self-assembly of the supramolecular spheres can be well-controlled by adjusting pH of the aqueous solution. As shown in the TEM image (Figure 2a), the supramolecular spheres assembled by Eu-POM and IL have a diameter of around 80−120 nm. Dynamic light scattering (DLS) measurement indicates the average diameter of these spheres is around 103 nm (Figure S1). Composition of these spheres was investigated to understand how they were formed in water. The elemental measurements indicate the exact stoichiometry between Eu-POM and IL is 1:6. The FTIR spectrum of Eu-POM exhibits four characteristic vibration bands at 942, 845, 787, and 709 cm^{-1} (Figure 2b, top).[36] It is noted that these bands shift in the FTIR spectrum of Eu-POM/IL hybrids (Figure 2b, bottom) due to electrostatic interactions and hydrogen bond between the molecular blocking components. In addition, the band corresponding to the carbonyl stretching vibration increase from 1729 cm^{-1} (Figure S2a) to 1739 cm^{-1} (Figure S2b) after formation of the hybrids, implying existence of hydrogen bond between Eu-POM and IL.[37] Hydrophobic interactions are analyzed to further study self-assembling behavior of Eu-POM and IL. Figure S2b shows presence of the $\nu_{as}(CH_2)$ and $\nu_s(CH_2)$ bands at 2924 and 2852 cm^{-1}, respectively, indicating the gauche conformer exists and hydrocarbon chains of ILs are relatively disordered.[27,38]

The UV−vis absorption spectrum shows strong characteristic peak of POMs at 203 nm (Figure S3a), corresponding to the O → W ligand-to-metal charge-transfer transition. For Eu-POM/IL hybrids, the absorption peak red-shifted to 210 nm (Figure S3b), which can be attributed to dense arrangement and identical orientation of the hydrophobic chains of ILs. The compact arrangements and identical orientation of the carbon chains make the big π-conjugated bonds of Eu-POM overlap partly. The big π-conjugated bond results in red-shift of absorption.[39] The SAXS diffractogram (Figure S4) demonstrates one obvious scattering peak. The calculated interplanar distance (d) is 3.83 nm. The energy minimized structures of [N-C_{12}, N′-COOH-Im]Br molecules at the B3LYP/6-31G(d,p) level are shown in Figure S5a, which demonstrates that the hydrophobic chain length of [N-C_{12}, N′-COOH-Im]Br is 1.69 nm. The width of POMs is 0.80 nm (Figure S5b). Thus, the theoretical layer spacing (d_{theory}) is 2.49 nm. Apparently, the calculated interplanar distance (d) based on SAXS pattern is larger than the theoretical layer spacing (d_{theory}) but less than twice its value. It may be originated from the cross-bedding stacking of [N-C_{12}, N′-COOH-Im]Br molecules in the theoretical calculation.

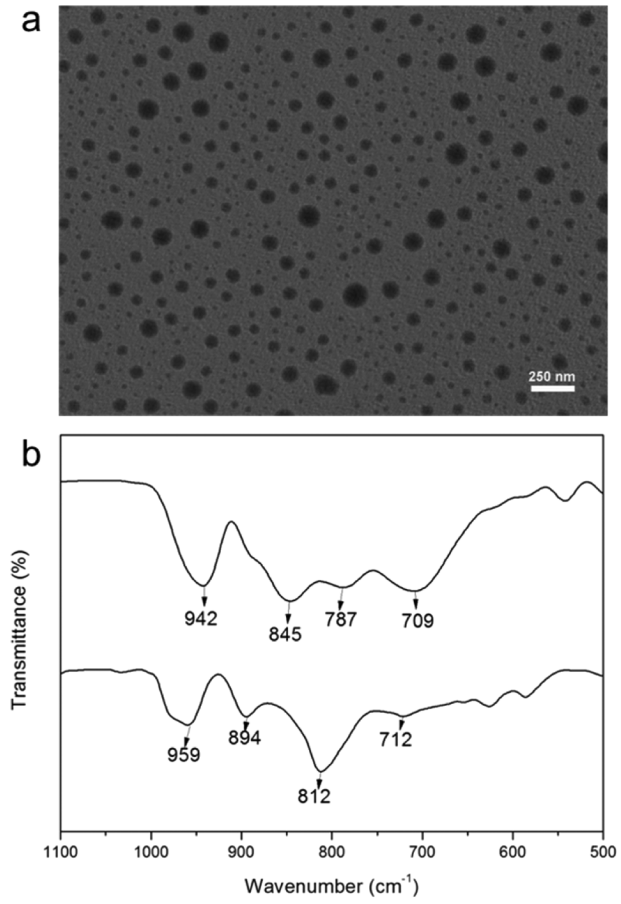

Figure 2. (a) TEM image of the Eu-POM-IL supramolecular spheres self-assembled at room temperature in water. (b) FTIR spectra of Eu-POM (top) and Eu-POM/[N-C_{12}, N′-COOH-Im] hybrids (bottom).

3.2. Reversible Stimuli-Responsive Self-Assembly and Photoluminescence Properties. Responsiveness to various external changes is a desirable feature for practical applications of self-assembled nanostructures. We found that change of pH could alter turbidity (Figure 3a) and fluorescence (Figure 3b) of the aqueous solution using a pH meter. Turbidity of the solution decreased with a progressive injection of NaOH (0.1 M). When pH was raised from 3.0 to 7.2, the solution became transparent finally, accompanied by complete dissociation of

DOI: 10.1021/acs.langmuir.5b03883
Langmuir 2016, 32, 421−427

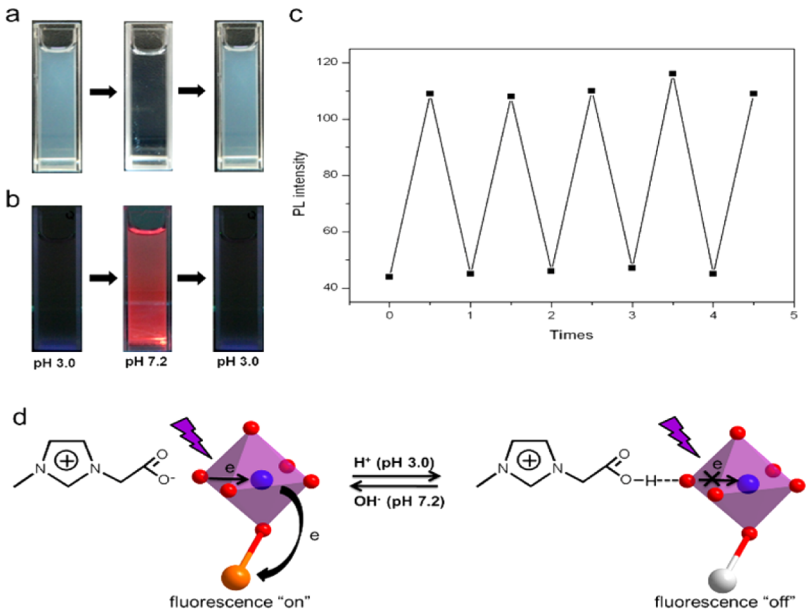

Figure 3. Photographs showing reversible (a) turbidimetric and (b) fluorescent responses of the Eu-POM/IL supramolecular spheres between pH 3.0 and 7.2 in water at an excitation wavelength of 254 nm. (c) Plot of fluorescence intensity of Eu-POM/IL supramolecular spheres upon five cycles of alternating pH between 3.0 and 7.2 at an excitation wavelength of 280 nm. (d) Mechanism for the pH-reversible fluorescence responses of the POM/IL supramolecular spheres.

the supramolecular spheres. However, turbidity of the solution was gradually restored after dropwise adding HCl (0.1 M). The cloudy system could be rebuilt by alternating the pH from 7.2 to 3.0, which made it possible to the circulation of materials. Additionally, the size of reassembled spheres was almost unchanged during the pH-reversible process (Figure S6). It is also interesting to observe that fluorescence of the supramolecular spheres could be well controlled by adjusting pH of the aqueous solution (Figure S7). It was completely quenched at pH 3.0 but was then recovered at pH 7.2. Eu-POM/IL hybrids emitted red fluorescence when excited by UV light mainly due to $^5D_0-^7F_j$ (j = 0, 1, 2, 3, 4) transitions of Eu^{3+}. The corresponding bands were observed at 580, 590, 620, 655, and 690 nm, respectively (Figure S7).[18] In addition, we found the photoluminescent switching behavior of the supramolecular spheres could also be reversibly modulated repeatedly between pH 3.0 and 7.2 (Figure 3c).

It has been well studied that Eu-POM displays a strong red emission due to intramolecular energy transfer from the POM molecule to Eu^{3+}.[36,40] The process can be divided into three steps. First, photoexcitation of the O → W ligand-to-metal charge transfer (LMCT) bands causes the hopping of the d_1 electron. Second, electron transfers from the O−W LMCT excited state to the $^5D_0$ emitting state of Eu^{3+}. Third, the electron originating from the $^5D_0$ excited state relaxes to the ^7F_j ground state, which ultimately generates the fluorescence. In our study, the fluorescence was quenched due to block of the first step. The hydrogen bond existing between Eu-POM and [N-C_{12}, N′-COOH-Im]Br acts as a bridge between the oxygen atom of POM and the carboxylic acid group of IL, which blocks hopping of the d_1 electron in the POM molecule (Figure 3d). Therefore, no photoluminescence was observed due to block of the electron transfer from POM to Eu^{3+}. In addition, we also conducted a control experiment by using [N-C_{12}, N′-Im]Br (Figure S8) to further study the effect of the carboxylic acid on fluorescence responses of the complexes. The Eu-POM/[N-C_{12}, N′-Im] hybrid materials were prepared by incubating the Eu-POM with [N-C_{12}, N′-Im]Br in water (Figure S9). It was observed that the Eu-POM/[N-C_{12}, N′-Im] hybrids only exhibited strong fluorescence emission without pH responses due to lack of the carboxylic acid group in [N-C_{12}, N′-Im]Br (Figure S10). This also proves that the hydrogen bond between the carboxylic acid group and Eu-POM is mainly responsible for the fluorescence quenching of Eu-POM. When pH was increased, the self-assembled supramolecular spheres disassembled. Thus, photoluminescence was observed due to disappearance of the hydrogen bond.

3.3. Potential Applications of the Stimuli-Responsive Eu-POM/IL Supramolecular Spheres. Urease is an enzyme that can hydrolyze urea into ammonia and carbon dioxide, thereby increasing pH of the aqueous solution. Because of its high stability and efficiency, it has been reported as a reporter molecule for detection of human pathogens such as *Helicobacter pylori* (Hp) and *Escherichia coli* (*E. coli*) based on pH changes of the aqueous solution.[41,42] In consideration of the sensitive pH responses of the fabricated Eu-POM/IL supramolecular spheres, we developed a simple and convenient approach with dual responses of turbidimetric and fluorescent signaling for the detection of urease. The aqueous solution containing Eu-POM/IL supramolecular spheres and 50 mM urea did not show obviously change when it was incubated for 0.5 h at room temperature. However, it gradually changed from cloudy to transparent within 1 min when a final concentration of 0.5 mg/mL urease was added into the aqueous solution.

Further decreasing concentrations of urease extended the time required for changing the solution from cloudy to transparent until the concentration of urease reached as low as 0.0005 mg/mL (Figure 4a). As heavy metals such as Cu^{2+} can block catalytic sites of urease,[41] we also examined responses of the system with Cu^{2+}-inhibited urease (0.05 mg/mL). In contrary to urease, decreasing concentrations of Cu^{2+} reduced the time required for changing the aqueous solution from cloudy to transparent, revealing the blocking effect of Cu^{2+} (Figure S11). Detection limit of the copper ions was around 0.5

DOI: 10.1021/acs.langmuir.5b03883
Langmuir 2016, 32, 421−427

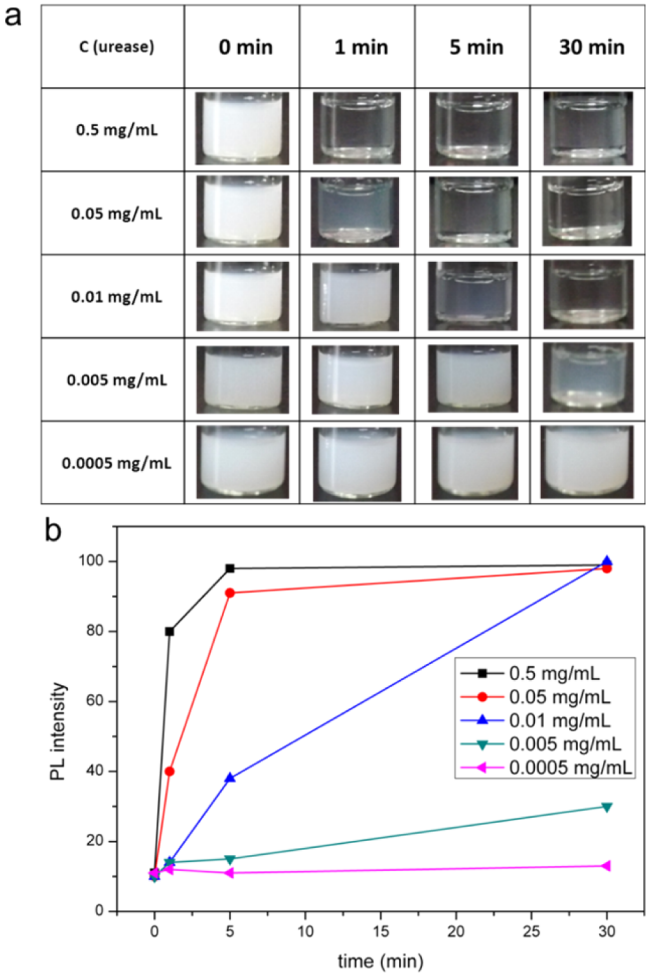

Figure 4. (a) Photographs showing turbidimetric changes of the POM/IL supramolecular spheres in aqueous phase upon addition of different concentrations of urease in the presence of 50 mM urea. (b) Fluorescence intensities of the Eu-POM/IL supramolecular spheres in aqueous solution of 50 mM urea upon incubation of different concentrations of urease for 30 min.

μM. In addition, we measured fluorescence of the aqueous solutions containing Eu-POM/IL supramolecular spheres after incubating different concentrations of urease (Figure 4b). Fluorescence intensities increased with raising concentrations of urease due to disassembly of the supramolecular spheres, consistent with the turbidity assay. These results suggest Eu-POM/IL supramolecular spheres could be applied in sensing applications based on the pH-induced turbidimetric and fluorescent responses.

In view of the reversible self-assembly behavior of the photoluminescent supramolecular spheres, we also studied feasibility of exploiting these supramolecular materials as carriers for controlled drug release by using methyl orange (MO) as a model molecule. The confocal laser scanning microscopy (CLSM) image shows the MO molecules could be incorporated into the supramolecular spheres as guests (Figure 5a). Addition of these supramolecular spheres into an aqueous solution of 0.5 mg/mL urease and 50 mM urea induced disassembly of the supramolecular spheres, leading to release of the entrapped dye molecules (Figure 5b). Similar results were also observed using the supramolecular spheres encapsulated with Rhodamine 6G (R6G) (Figure S12). These results suggest

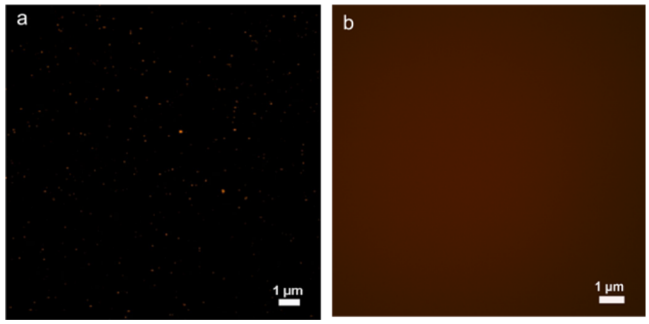

Figure 5. CLSM images of (a) the supramolecular sphere encapsulated with MO molecules and (b) trapped dye molecules released in the aqueous solution of 0.5 mg/mL urease and 50 mM urea within 5 min at an excitation wavelength of 380 nm.

Eu-POM/IL hybrids can also be applied as carriers for the study of controlled drug release, which is an important feature for potential *in vivo* applications.

4. CONCLUSIONS

In summary, this study demonstrates fabrication, characterization, and potential applications of stimuli-responsive Eu-POM/IL supramolecular spheres exhibiting excellent pH-reversible self-assembly and adjustable photoluminescent properties in aqueous solution. Electrostatic interactions, hydrogen bond, and hydrophobic interactions are the main driving forces for the formation of these supramolecular spheres with highly ordered structures. Noteworthy is that turbidimetric and fluorescent assays were applied simultaneously in the study of biochemical interactions. In addition, controlled release of the encapsulated guest molecules from the supramolecular spheres was fulfilled in the presence of external stimuli. This study reveals potential of stimuli-responsive Eu-POM/IL supramolecular materials in biological applications.

■ ASSOCIATED CONTENT

Supporting Information

The Supporting Information is available free of charge on the ACS Publications website at DOI: 10.1021/acs.langmuir.5b03883.

Figures S1−S12 (PDF)

■ AUTHOR INFORMATION

Corresponding Author

*Phone +86-531-88364807; Fax +86-531-88564750; e-mail ylmlt@sdu.edu.cn (L.Y.).

Author Contributions

Y.G. and Q.H. made equal contributions.

Notes

The authors declare no competing financial interest.

■ ACKNOWLEDGMENTS

This work was supported by the National Natural Science Foundation of China (No. 21373128), the Scientific and Technological Projects of Shandong Province of China (No. 2014GSF117001), and the China Scholarship Council (CSC).

DOI: 10.1021/acs.langmuir.5b03883
Langmuir 2016, 32, 421−427

REFERENCES

(1) Hartgerink, J. D.; Beniash, E.; Stupp, S. I. Self-assembly and mineralization of peptide amphiphile nanofibers. *Science* **2001**, *294*, 1684−1688.

(2) Jonkheijm, P.; van der Schoot, P.; Schenning, A. P.; Meijer, E. W. Probing the solvent assisted nucleation pathway in chemical self-assembly. *Science* **2006**, *313*, 80−83.

(3) Grzelczak, M.; Vermant, J.; Furst, E. M.; Liz-Marzán, L. M. Directed self-assembly of nanoparticles. *ACS Nano* **2010**, *4*, 3591−3605.

(4) Del Borgo, M. P.; Mechler, A. I.; Traore, D.; Forsyth, C.; Wilce, J. A.; Wilce, M. C. J.; Aguilar, M. I.; Perlmutter, P. Supramolecular self-assembly of N-Acetyl-Capped β-Peptides leads to nano- to macroscale fiber formation. *Angew. Chem., Int. Ed.* **2013**, *52*, 8266−8270.

(5) Faul, C. F. J.; Antonietti, M. Ionic self-assembly: Facile synthesis of supramolecular materials. *Adv. Mater.* **2003**, *15*, 673−683.

(6) Zhang, X.; Zou, J.; Tamhane, K.; Kobzeff, F. F.; Fang, J. Self-assembly of pH-switchable spiral tubes: supramolecular chemical springs. *Small* **2010**, *6*, 217−220.

(7) Wang, C.; Chen, Q.; Xu, H.; Wang, Z.; Zhang, X. Photo-responsive supramolecular amphiphiles for controlled self-assembly of nanofibers and vesicles. *Adv. Mater.* **2010**, *22*, 2553−2555.

(8) Han, J.-M.; Xu, M.; Wang, B.; Wu, N.; Yang, X.; Yang, H.; Salter, B. J.; Zang, L. Low dose detection of γ-radiation via solvent assisted fluorescence quenching. *J. Am. Chem. Soc.* **2014**, *136*, 5090−5096.

(9) Fenske, M. T.; Meyer-Zaika, W.; Korth, H. G.; Vieker, H.; Turchanin, A.; Schmuck, C. Cooperative self-assembly of discoid dimers: hierarchical formation of nanostructures with a pH switch. *J. Am. Chem. Soc.* **2013**, *135*, 8342−8349.

(10) Yan, X.; Zhu, P.; Fei, J.; Li, J. Self-assembly of peptide-inorganic hybrid spheres for adaptive encapsulation of guests. *Adv. Mater.* **2010**, *22*, 1283−1287.

(11) Kamata, K.; Yonehara, K.; Nakagawa, Y.; Uehara, K.; Mizuno, N. Efficient stereo- and regioselective hydroxylation of alkanes catalysed by a bulky polyoxometalate. *Nat. Chem.* **2010**, *2*, 478−483.

(12) Chen, C.; Wang, Q.; Lei, P.; Song, W.; Ma, W.; Zhao, J. Photodegradation of dye pollutants catalyzed by porous K3PW12O40 under visible irradiation. *Environ. Sci. Technol.* **2006**, *40*, 3965−3970.

(13) Nisar, A.; Lu, Y.; Zhuang, J.; Wang, X. Polyoxometalate nanocone nanoreactors: Magnetic manipulation and enhanced catalytic performance. *Angew. Chem., Int. Ed.* **2011**, *50*, 3187−3192.

(14) Wang, J.; Han, D.; Wang, X.; Qi, B.; Zhao, M. Polyoxometalates as peroxidase mimetics and their applications in H_2O_2 and glucose detection. *Biosens. Bioelectron.* **2012**, *36*, 18−21.

(15) Li, W.; Yin, S.; Wang, J.; Wu, L. Tuning mesophase of ammonium amphiphile-encapsulated polyoxometalate complexes through changing component structure. *Chem. Mater.* **2008**, *20*, 514−522.

(16) He, P.; Xu, B.; Liu, H.; He, S.; Saleem, F.; Wang, X. Polyoxometalate-based supramolecular gel. *Sci. Rep.* **2013**, *3*, 1833−1838.

(17) Bu, W.; Uchida, S.; Mizuno, N. Micelles and vesicles formed by polyoxometalate-block copolymer composites. *Angew. Chem., Int. Ed.* **2009**, *48*, 8281−8284.

(18) Landsmann, S.; Luka, M.; Polarz, S. Bolaform surfactants with polyoxometalate head groups and their assembly into ultra-small monolayer membrane vesicles. *Nat. Commun.* **2012**, *3*, 1299−1304.

(19) Jin, Y.; Bi, L.; Shao, Y. Robust core-shell supramolecular assemblies based on cationic vesicles and ring-shaped {Mo154} polyoxomolybdate nanoclusters: template-directed synthesis and characterizations. *Chem. - Eur. J.* **2004**, *10*, 3225−3231.

(20) Li, H.; Sun, H.; Qi, W.; Xu, M.; Wu, L. Onionlike hybrid assemblies based on surfactant-encapsulated polyoxometalates. *Angew. Chem., Int. Ed.* **2007**, *46*, 1300−1303.

(21) Rickert, P. G.; Antonio, M. R.; Firestone, M. A.; Kubatko, K. A.; Szreder, T.; Wishart, J. F.; Dietz, M. L. Tetraalkylphosphonium polyoxometalate ionic liquids: Novel, organic-inorganic hybrid materials. *J. Phys. Chem. B* **2007**, *111*, 4685−4692.

(22) Li, H.; Qi, W.; Li, W.; Sun, H.; Bu, W.; Wu, L. A highly transparent and luminescent hybrid based on the copolymerization of surfactant-encapsulated polyoxometalate and methyl methacrylate. *Adv. Mater.* **2005**, *17*, 2688−292.

(23) Nisar, A.; Zhuang, J.; Wang, X. Cluster-based self-assembly: Reversible formation of polyoxometalate nanocones and nanotubes. *Chem. Mater.* **2009**, *21*, 3745−3751.

(24) Yang, Y.; Zhang, B.; Wang, Y.; Yue, L.; Li, W.; Wu, L. A photo-driven polyoxometalate complex shuttle and its homogeneous catalysis and heterogeneous separation. *J. Am. Chem. Soc.* **2013**, *135*, 14500−14503.

(25) Yan, Y.; Wang, H.; Li, B.; Hou, G.; Yin, Z.; Wu, L.; Yam, V. W. Smart self-assemblies based on a surfactant-encapsulated photo-responsive polyoxometalate complex. *Angew. Chem., Int. Ed.* **2010**, *49*, 9233−9236.

(26) Bai, T.; Ge, R.; Gao, Y. The effect of water on the microstructure and properties of benzene/[bmim][AOT]/[bmim]-[BF_4] microemulsions. *Phys. Chem. Chem. Phys.* **2013**, *15*, 19301−19311.

(27) Geisberger, G.; Gyenge, E. B.; Hinger, D.; Bösiger, P.; Maake, C.; Patzke, G. R. Synthesis, characterization and bioimaging of fluorescent labeled polyoxometalates. *Dalton Trans.* **2013**, *42*, 9914−9920.

(28) Zhang, T.; Spitz, C.; Antonietti, M.; Faul, C. F. Highly photoluminescent polyoxometaloeuropate-surfactant complexes by ionic self-assembly. *Chem. - Eur. J.* **2005**, *11*, 1001−1009.

(29) Zhang, H.; Lin, X.; Yan, Y.; Wu, L. Luminescent logic function of a surfactant-encapsulated polyoxometalate complex. *Chem. Commun.* **2006**, 4575−4577.

(30) Liu, S.; Tian, J.; Wang, L.; Zhang, Y.; Luo, Y.; Li, H.; Asiri, A. M.; Al-Youbi, A. O.; Sun, X. Fast and sensitive colorimetric detection of H_2O_2 and glucose: a strategy based on polyoxometalate clusters. *ChemPlusChem.* **2012**, *77*, 541−544.

(31) Babakhanian, A.; Kaki, S.; Ahmadi, M.; Ehzari, H.; Pashabadi, A. Development of α-polyoxometalate-polypyrrole-Au nanoparticles modified sensor applied for detection of folic acid. *Biosens. Bioelectron.* **2014**, *60*, 185−190.

(32) Fu, L.; Gao, H.; Yan, M.; Li, S.; Li, X.; Dai, Z.; Liu, S. Polyoxometalate-based organic-inorganic hybrids as antitumor drugs. *Small* **2015**, *11*, 2938−2945.

(33) Wei, H.; Zhang, J.; Shi, N.; Liu, Y.; Zhang, B.; Zhang, J.; Wan, X. recyclable polyoxometalate-based supramolecular chemosensor for efficient detection of carbon dioxide. *Chem. Sci.* **2015**, *6*, 7201−7205.

(34) Wang, X.; Liu, J.; Yu, L.; Jiao, J.; Wang, R.; Sun, L. Surface adsorption and micelle formation of imidazolium-based zwitterionic surface active ionic liquids in aqueous solution. *J. Colloid Interface Sci.* **2013**, *391*, 103−110.

(35) Sugeta, M.; Yamase, T. Crystal structure and luminescence site of $Na_9(EuW_{10}O_{36})$ $32H_2O$. *Bull. Chem. Soc. Jpn.* **1993**, *66*, 444−449.

(36) Wang, Z.; Zhang, R.; Ma, Y.; Peng, A.; Fu, H.; Yao, J. Chemically responsive luminescent switching in transparent flexible self-supporting $[EuW_{10}O_{36}]_9$–agarose nanocomposite thin films. *J. Mater. Chem.* **2010**, *20*, 271−277.

(37) Leng, Y.; Wang, J.; Zhu, D.; Zhang, M.; Zhao, P.; Long, Z.; Huang, J. Polyoxometalate-based amino-functionalized ionic solid catalysts lead to highly efficient heterogeneous epoxidation of alkenes with H_2O_2. *Green Chem.* **2011**, *13*, 1636−1639.

(38) Gong, Y.; Hu, Q.; Cheng, N.; Wang, T.; Xu, W.; Bi, Y.; Yu, L. Fabrication of pH-and temperature-directed supramolecular materials from 1D fibers to exclusively 2D planar structures using an ionic self-assembly approach. *J. Mater. Chem. C* **2015**, *3*, 3273−3279.

(39) Zhang, T. R.; Feng, W.; Fu, Y. Q.; Lu, R.; Bao, C. Y.; Zhang, X. T.; Zhao, B.; Sun, C. Q.; Li, T. J.; Zhao, Y. Y.; Yao, J. N. Self-assembled organic−inorganic composite superlattice thin films incorporating photo-and electro-chemically active phosphomolybdate anion. *J. Mater. Chem.* **2002**, *12*, 1453−1458.

(40) Wang, X.; Wang, J.; Tsunashima, R.; Pan, K.; Cao, B.; Song, Y.-F. Electrospun self-supporting nanocomposite films of

DOI: 10.1021/acs.langmuir.5b03883
Langmuir 2016, 32, 421−427

$Na_9[EuW_{10}O_{36}]\cdot 32H_2O$/PAN as pH-modulated luminescent switch. *Ind. Eng. Chem. Res.* **2013**, *52*, 2598−2603.
(41) Hu, Q. Z.; Jang, C. H. Liquid crystal-based sensors for the detection of heavy metals using surface-immobilized urease. *Colloids Surf., B* **2011**, *88*, 622−626.
(42) Tram, K.; Kanda, P.; Salena, B. J.; Huan, S.; Li, Y. Translating bacterial detection by DNAzymes into a litmus test. *Angew. Chem., Int. Ed.* **2014**, *53*, 12799−12802.

DOI: 10.1021/acs.langmuir.5b03883
Langmuir 2016, 32, 421−427